On the role of stacking fault energy in the hydrogen embrittlement sensitivity of twinning induced plasticity (TWIP) steel

Lisa Claeys[1], **Tom Depover**[1], **Kim Verbeken**[1]

[1]*Ghent University, Department of Materials, Textiles and Chemical Engineering, Research group Sustainable Materials Science, Ghent, Belgium, lisa.claeys@ugent.be; tom.depover@ugent.be; kim.verbeken@ugent.be*

Abstract: Aluminium addition is claimed to improve the hydrogen embrittlement (HE) resistance of twinning-induced plasticity (TWIP) steels. The associated increase in stacking fault energy (SFE) is one of the proposed mechanisms since a higher SFE decreases twinning leading to less crack initiation sites. The objective of this work is to increase knowledge on the HE resistance improvement with aluminium addition by excluding the SFE parameter. For this purpose, an Fe-18Mn-0.6C TWIP steel is compared to Fe-18Mn-0.6C-1.5Al and a third TWIP steel with equal SFE as the aluminium added variant by increasing the manganese content (Fe-24.5Mn-0.6C). The hydrogen content increases with the aluminium and manganese additions after electrochemical hydrogen charging. Moreover, it is found that the aluminium addition decreases the hydrogen diffusivity slightly. Ex-situ constant extension rate tensile tests with and without hydrogen precharging are executed to quantify the embrittlement and to assess post-mortem the deformation behaviour by SEM-EBSD characterization. Aluminium addition clearly results in a reduced HE sensitivity. Manganese addition, however, increases the HE sensitivity. This suggests that the SFE is not the main factor controlling the HE sensitivity in the present work. The resistance to intergranular cracking rather determines the ranking of the HE sensitivities.

Keywords: Twinning-induced plasticity steel, Hydrogen embrittlement, Stacking fault energy, Electron backscatter diffraction, Deformation

Introduction

Twinning-induced plasticity (TWIP) steels are high manganese steels with an austenitic crystal structure in which deformation is driven by twin formation. As a result, TWIP steels are characterized by a high ultimate strength while maintaining a significant level of ductility, making them excellent candidate materials for structural parts in cars [1, 2]. TWIP steels are, however, prone to delayed cracking, which is governed by the uptake of hydrogen and the presence of high residual tensile stresses. This phenomenon is closely related to hydrogen embrittlement (HE), i.e. the loss of mechanical properties due to the presence of hydrogen in the microstructure [3]. Despite numerous attempts, the underlying mechanism of HE and delayed cracking in TWIP steels has not yet been elucidated [4].

Addition of aluminium (Al) to TWIP steels was reported to have a beneficial effect on the HE sensitivity of TWIP steels [4]. A number of mechanisms have been proposed to explain the role of Al. Firstly, the increase of the stacking fault energy (SFE) by Al is stated to reduce the possibility for α'-martensite, ε-martensite and twin formation, which is in correspondence with the theory that these features are responsible for hydrogen-induced damage initiation [5]. In a second mechanism, Al is stated to suppress dynamic strain aging (DSA) making the material less strong and thus less HE sensitive [6, 7]. In a third mechanism, Al is supposed to reduce the absorption of H [8, 9]. In a final mechanism, Al enhanced the H absorption but reduced the H diffusion [10, 11]. The latter two proposed mechanisms are contradictive to each other in terms of the amount of absorbed hydrogen. The number of proposed mechanisms in literature indicates that agreement on the role of Al is far from reached and, therefore, requires further investigation.

Materials and methods

Three different TWIP steels were cast. The steels were hot rolled at 1100°C with heating in between the passes and subsequently water quenched. An Fe-18Mn-0.6C TWIP steel (18Mn) served as reference alloy. The addition of Al was achieved in a Fe-18Mn-0.6C-1.5Al alloy (1.5Al). In order to exclude the SFE parameter from the study, Fe-24.5Mn-0.6C (24.7Mn) was cast as well since the increase in Mn content increased the SFE to an equal value as the Fe-18Mn-0.6C-1.5Al TWIP steel. The SFE of the alloys was calculated using the thermodynamic model given in [12]. For the calculations, a constant interfacial energy of 15 mJ/m² was assumed.

Table 1: Thermodynamically calculated SFE based on values from [12]

TWIP alloy	Fe-18Mn-0.6C	Fe-18Mn-0.6C-1.5Al	Fe-24.5Mn-0.6C
SFE [mJ/m²]	16.24	29.63	30.40

Characterization of the materials was done with scanning electron microscopy (SEM). A FEI Quanta-450 FEG SEM was used for this purpose operated with an accelerating voltage of 20 kV and a spot size of 5 nm. The surfaces were prepared with electropolishing in Struers A2 electrolyte at 35V for six seconds. Electrochemical hydrogen charging was performed in an electrolyte of 1.31 mol/l sodium tetraborate decahydrate ($Na_2B_4O_7.10H_2O$) in glycerol ($C_3H_8O_5$) at 5 mA/cm² for 7 days. To reach an adequate conductivity, 20 vol% of distilled water was added. The solution was used at a temperature of 50°C. The hydrogen content was measured via thermal desorption spectroscopy (TDS) measurements at a constant heating rate of 600°C/h. The specimen thickness was reduced to 0.2 ± 0.01 mm to reach near saturation if the charging temperature was increased to 80°C. In previous work, it was shown that diffusion is the rate-determining step during hydrogen desorption from austenitic steels in TDS measurements. Hence, the hydrogen solubility and diffusivity were both evaluated using the method described in [13]. To evaluate the influence of hydrogen on the mechanical properties of the three TWIP steels, tensile tests were performed in an Instron 5800R electromechanical bench at a constant strain rate of $5x10^{-5}$ s^{-1}. The geometry of the specimens can be found in Figure 1. The specimens were ground to a thickness of 0.7 ± 0.01 mm. The surfaces were finished with 1 µm polishing. Both hydrogen precharged and reference specimens were tested in air. The former was executed immediately after the charging procedure. It should be noted that the tensile specimens were heterogeneously charged with hydrogen showing a high surface hydrogen concentration. Electron backscatter diffraction (EBSD) was used to study deformation mechanisms and hydrogen-assisted cracking on intermediately interrupted tensile tested specimens. The specimen was additionally polished up to 0.05 µm (OP-U) after tensile testing and tilted to 70° inside the SEM. The step size was 0.2 µm on a hexagonal grid.

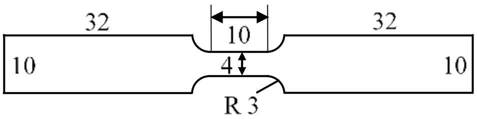

Figure 1: Tensile geometry (numbers in millimeter).

Results and discussion

Figure 2 shows SE images of the three TWIP steels. The grains were equiaxed and several annealing twins were present. The grain size of the 1.5Al alloy was slightly higher: on average 22.6 µm compared to 17.4 µm for 18Mn and 16.9 µm for 24.5Mn.

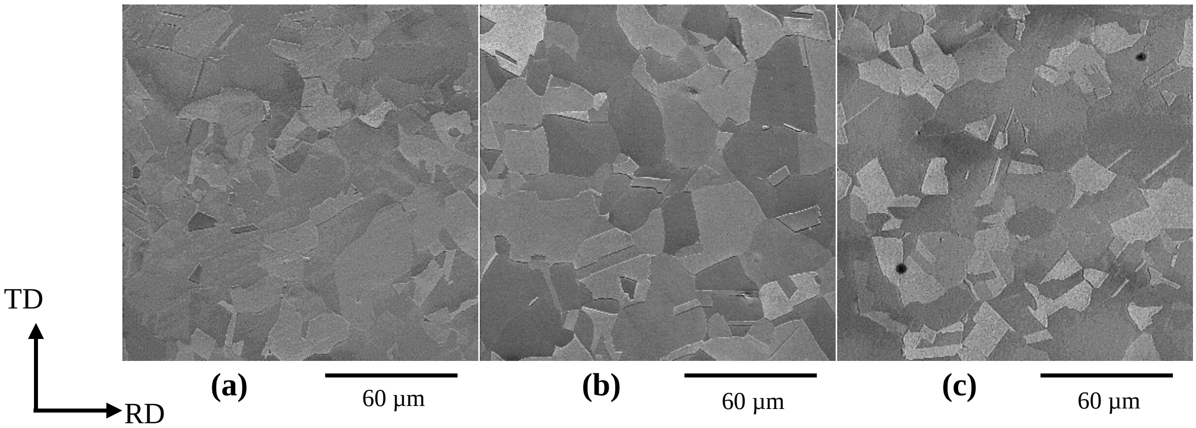

Figure 2: SE image of the microstructure of (a) 18Mn, (b) 1.5Al and (c) 24.5Mn TWIP steel.

The TDS results are presented in Figure 3 (left image). The results show one main asymmetrical peak resulting from hydrogen diffusion as being the rate-determining step. The analysis results obtained with the model developed in [13] is also presented in Figure 3 (right image). The 18Mn TWIP steel clearly had a lower hydrogen solubility compared to the other materials, i.e. both the addition of aluminium and manganese increased the hydrogen solubility and thus the number of hydrogen trapping sites. Secondly, the hydrogen diffusivity was slightly reduced by the addition of aluminium, while manganese increased the diffusivity compared to the reference 18Mn TWIP steel. The difference is, however, minimal.

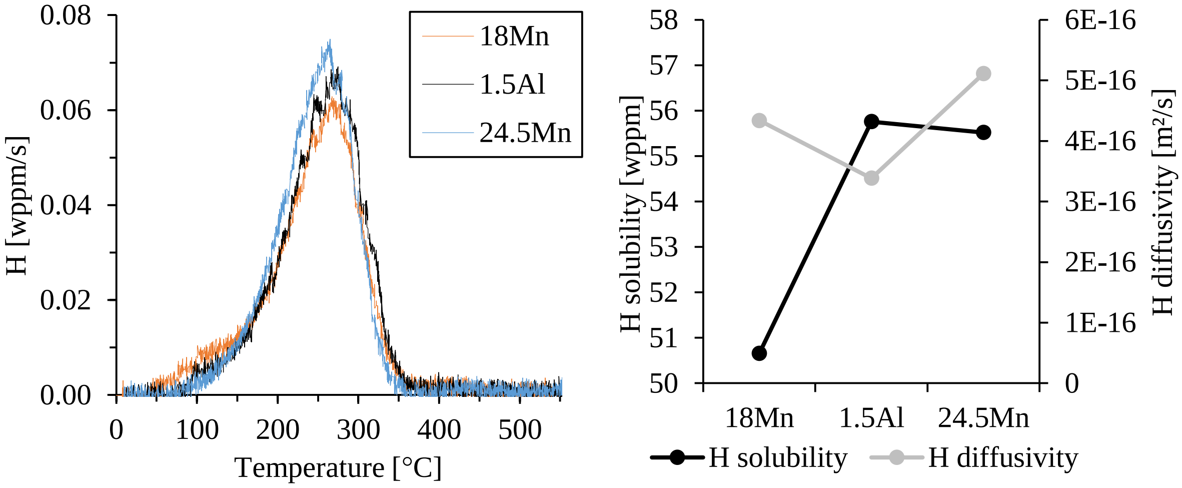

Figure 3: TDS spectra (heating rate 600 °C/h) of the three TWIP steels (left) and derived H solubility and diffusivity evaluated at room temperature (right).

Constant extension rate tensile tests were performed to evaluate the HE sensitivity of the three TWIP steels. In Table 2, the average ultimate tensile strength (UTS) and engineering strain at fracture are given for all materials with and without hydrogen precharging. The engineering stress was calculated as the load applied to the specimen divided by the initial cross-sectional area, while the crosshead displacement and initial gauge length were used for the calculation of the engineering strain. DSA was observed as serrations on the engineering stress/strain curves and can be related to the short range reorientation of C-Mn complexes and their interaction with stacking faults enclosed by partial dislocations [14]. The DSA is decreased in the case of 1.5Al since Al decreases the carbon activity [15]. This might explain the slightly lower UTS of 1.5Mn compared to 24.5Mn, although the SFE was similar and should thus result in similar deformation twinning. With hydrogen precharging, a clear reduction in UTS and strain at fracture is observed for all TWIP steels. Table 2 additionally shows the embrittlement index for the three TWIP steels, calculated based on the engineering strain at fracture. Al addition clearly improved the HE resistance compared to the reference 18Mn TWIP steel, despite its higher hydrogen solubility. Mn addition, on the contrary, reduced the HE resistance, most likely aided by the higher H solubility and diffusivity compared to 18Mn TWIP steel. These results indicate that the SFE was not the determining factor in the HE sensitivity of the TWIP steels in the present work.

Table 2: Average UTS and strain at fracture for the three TWIP steels with and without hydrogen, embrittlement index based on engineering strain at fracture

	UTS [MPa]		Engineering strain at fracture [%]		Embrittlement index [%]
	Air	H	Air	H	
18Mn	1058 ± 14	850 ± 28	106.1 ± 1.6	61.9 ± 3.7	41.7 ± 1.8
1.5Al	894 ± 9	769 ± 23	93.5 ± 4.7	58.2 ± 1.6	37.7 ± 3.5
24.5Mn	935 ± 5	698 ± 21	97.5 ± 2.5	51.3 ± 2.3	47.4 ± 2.6

EBSD phase maps on intermediately interrupted tensile tested specimens with precharged hydrogen further reveal the acting deformation mechanisms in these materials. Tensile tests were interrupted at an engineering strain level of 30%. The 18Mn TWIP steel showed hydrogen-induced ε-martensitic transformation combined with deformation twinning, while the other two TWIP steels only showed extensive deformation twinning. The difference in deformation mechanisms can be directly related to the different SFE where the lower SFE of the 18Mn steel enables martensitic transformations. Moreover, the higher the manganese content, the more hydrogen-induced cracks (HACs) were observed. The cracks mainly had an intergranular character propagating along high angle grain boundaries (HAGB), which can be linked to the reduction in the cohesive strength of grain boundaries with increasing manganese content for TWIP steels [16]. It should be noted that the presence of hydrogen is required since no cracks were observed on the air tested specimens. In contradiction to the TWIP steels with only manganese addition, the fraction of HACs was low in the 1.5Al TWIP steel, i.e. aluminium reduced the amount of possible crack initiation sites. This reduced cracking sensitivity in the presence of hydrogen most likely explains the reduced HE sensitivity when Al is added. A more elaborate discussion on this can be found elsewhere [17].

Conclusions

It was shown that the addition of aluminium reduced the HE sensitivity of TWIP steel, while the addition of manganese increased it, despite similar SFEs. Both element additions increased the hydrogen solubility. The hydrogen diffusivity was not altered significantly. This could be concluded based on the combined experimental/numerical TDS analysis. Hydrogen-assisted cracking was most pronounced in the manganese added TWIP steel which was related to the high angle grain boundaries being prone to crack initiation in the presence of excess manganese. The effect of the SFE should be evaluated in TWIP steels with similar grain boundary cohesive strength in the presence of hydrogen or via mechanical testing at a length scale where the presence of grain boundaries could be eliminated.

Acknowledgement

The authors would like to acknowledge support from the FWO (SB PhD fellow grant no. 1S16620N and senior postdoctoral fellow grant no. 12ZO420N) and from the special research fund (BOF) of Ghent University (grant no. BOF15/BAS/062). The authors wish to thank prof. Hauke Springer (RWTH Aachen University and MPIE Düsseldorf) for the supply of the TWIP alloys.

References

1. B. De Cooman, Y. Estrin and S. Kim, Acta materialia, **142** (2018) 283.
2. O. Bouaziz, S. Allain, C. Scott, P. Cugy and D. Barbier, Current opinion in solid state and materials science, **15** (2011) 141.
3. M. Koyama, E. Akiyama, Y.-K. Lee, D. Raabe and K. Tsuzaki, International journal of hydrogen energy, **42** (2017) 12706.
4. D.-W. Suh, Materials Science and Technology, **30** (2014) 1131.
5. M. Koyama, E. Akiyama, K. Tsuzaki and D. Raabe , Acta materialia, **61** (2013) 4607.
6. M. Koyama, E. Akiyama and K. Tsuzaki, ISIJ international, **53** (2013) 1268.
7. H. K. D. H. Bhadeshia, ISIJ International, **56** (2016) 24.
8. I.-J. Park, K.-H. Jeong, J.-G. Jung, C. S. Lee and Y.-K. Lee, International journal of hydrogen energy, **37** (2012) 9925.
9. M. Koyama, E. Akiyama and K. Tsuzaki, ISIJ international, **52** (2012) 2283.
10. E. Song, H. Bhadeshia and D.-W. Suh, Scripta Materialia, **87** *(*2014) 9.
11. D. Han, S. Lee, S. Noh, S.-K. Kim and D.-W. Suh, Scripta materialia, **99** (2015) 45.
12. A. Saeed-Akbari, J. Imlau, U. Prahl and W. Bleck, Metallurgical and materials transactions A, **40** (2009) 3076.
13. L. Claeys, V. Cnockaert, T. Depover, I. De Graeve and K. Verbeken, Acta materialia, **186** (2020) 190.
14. S.-J. Lee, J. Kim, S. Kane and B. De Cooman, Acta materialia, **59** (2011) 6809.
15. T. Shun, C. Wan and J. Byrne, Acta metallurgica et materialia, **40** (1992) 3407.
16. M. Kuzmina, D. Ponge and D. Raabe, Acta materialia, **86** (2015) 182.
17. L. Claeys, T. Depover and K. Verbeken, to be published (2022)